



MADRID
inter.noise 2019
June 16 - 19

NOISE CONTROL FOR A BETTER ENVIRONMENT

Mechanism analysis of ice damage under underwater near-field explosion

Zhou, Peng¹

School of Mechanical and Electrical Engineering, Harbin Engineering University
Harbin, China;

Zhu, Shifan²

School of Mechanical and Electrical Engineering, Harbin Engineering University
Harbin, China;

ABSTRACT

In order to explore the dynamic response process of underwater explosion to ice layer, the CEL algorithm is used to establish the underwater explosion-ice layer and bubble-ice dynamic response model to study the dynamic load characteristics of underwater explosion shock wave and bubble, and the ice under the corresponding load. Layer dynamic response and damage characteristics. The results show that the shock wave load is higher than the bubble load, but the load pulse width is lower; the damage to the ice layer during the explosion shock wave stage can be divided into the ice free surface tensile failure caused by the stress wave unloading, and The impact surface collapse due to excessive shock wave failure. The bubble stage damage can be divided into the failure of the ice layer free surface caused by the bubble burst shock wave and the jet, and the penetration failure of the burst surface. The shock wave phase is the main stage of ice damage, and the back damage surface tensile damage is the main form of ice material damage. The bubble stage is the secondary stage of ice damage, and the impact surface penetration damage is a secondary form of ice material damage.

Keywords : Underwater Explosion; Ice layer, Damage Mechanism

Introduction

As one of the main methods to deal with the Yellow River ice blast disaster, the blasting method deicing has been widely used in view of its convenient construction characteristics^[1], and the damage of ice materials caused by underwater explosion has become the focus of many researchers. Due to the extremely short reaction time of the explosion detonation process, the impact equivalent is large, the detonation load is complex, and the ice material is a very special solid medium with non-uniformity, anisotropy, corresponding variability and temperature sensitivity^{[2][3]}, causing damage to ice materials under explosive conditions is an extremely complex process. Under the existing experimental equipment and testing methods, it is impossible to completely and accurately observe the damage process of the non-uniform stress-strain field caused by the explosion of the meso-level structure of the ice medium. The existing research is mostly based on experiments^{[4][5]}. With the development of computer technology and

¹ 924460904@qq.com

² zhushifan@hrbeu.edu.cn

observation technology, the maturity of numerical simulation technology enables researchers to observe the damage process of ice layer in a more detailed and accurate way.

The damage of the ice material during the detonation process is currently roughly divided into two stages: the shock wave damage stage and the bubble damage stage. In the study of the shock wave damage stage, some researchers have used numerical simulation methods. Qu Yandong et al^[6] studied the propagation law of underwater blasting icebreaking shock wave by acoustic-solid coupling algorithm, and macroscopically calculated the propagation process of explosive shock wave between ice layer and water body. Wang Huhe et al^[7] used the damage accumulation model to study the mechanism of explosive crack propagation in infinite ice media. Zhang Zhonghe et al^[8] used the brittle fracture theory to give the macroscopic damage mechanism of the ice shock wave stage. For the bubble damage phase, the bubble ruptures under conditions of internal and external pressure imbalance, during which various forms of dynamic properties, such as jets, shock waves and even light, are produced, and thereby erosion and fracture of the ice material. Fipppt & Loutern et al.^[9] showed that the damage pit was formed on the surface of the material exposed to a single burst bubble. As the distance of the bubble from the material changed, the damage pit gradually evolved from a dot to a ring, indicating that the damage and bubble collapse. The shock wave generated in the process is related to the jet. Hsiao et al^[10] and Chahine et al^[11] numerical simulations indicate that the pressure load on the surface of the material is mainly caused by the jet impact and the collapse of the remaining bubble ring. At present, many scholars use high-speed photography technology to observe the bubbles produced by EDM^[12]. Wang Ying et al^[13] numerically calculated and combined with the gray theory, gave the influence of different parameters on the ice layer explosion. Pu Cui et al^[14] observed the damage of air bubbles on ice trays under different dimensionless distances by high-speed photography. Xiongwei Cui et al^[15] applied the Hopkinson rod (HPB) as a sensor to measure the wall pressure under underwater explosion conditions. Yingyu Chen et al^[16] studied the dynamic behavior of bubbles and the pressure in the center of the wall through experimental methods and numerical studies. Liu, L. T, et al.^[17] gave empirical formulas for estimating various parameters of underwater explosion jets through experimental and numerical studies.

None of the above studies involved the internal stress distribution, damage form, damage mechanism and the damage degree of the two stages in the shock wave damage stage and the bubble damage stage. Therefore, this paper establishes the shock wave-ice layer coupling model and the bubble-ice layer coupling model respectively to study the ice damage process under the near-field conditions underwater explosion shock wave and bubble, and the two-stage damage form and damage mechanism. The comparison and summary provide a certain reference for the design of the explosion icebreaking scheme in the future.

1. Establishment of damage model for ice layer during detonation

1.1. Model material parameters

(1)Ice layer

The ice material adopts the Johnson-Holmquist model constitutive model, in which the damage model part adopts the cumulative damage model. The parameters of the constitutive model are shown in Table 1, and the parameters are close to the mechanical properties of fresh water ice at -15 °C.

Tab.1 Model parameters of ice material

Non-damage material strength coefficient A	Fracture material strength coefficient B	Material strain rate coefficient C	Fracture strength index coefficient M	Non-damage strength index coefficient N	EPSI Reference strain rate	Tensile Strength /GPa
0.93	0.088	0.003	0.35	0.77	1.0	0.15
Fracture stress / GPa	HEL Elastic limit / GPa	HEL Pressure / GPa	HEL Volume strain	HEL Strength / GPa	Damage constant D_1	Damage constant D_2
0.0003	5.95	2.92	0.02	4.5	0.053	0.85

(2)Air

Due to the anti-expansion characteristics of water, the ice layer is at the junction of water and air, and the air needs to be simulated during the calculation process. Air is simulated using the Ideal Gas Equation .The parameters are shown in Table 2.

Tab.2 Air state equation parameters

$\rho/g \cdot cm^{-3}$	Adiabatic coefficient	Bienergy/ $kJ \cdot kg^{-1}$	Air internal energy/J
1.225×10^{-3}	1.4	2.06785×10^5	2.068×10^5

(3) Explosive

The JWL equation of state is used to describe the process of detonation and volume change of detonation products of TNT explosives.

$$p = A\left(1 - \frac{\omega}{R_1 \bar{V}}\right)e^{-R_1 \bar{V}} + B\left(1 - \frac{\omega}{R_2 \bar{V}}\right)e^{-R_2 \bar{V}} + \frac{\omega E}{\bar{V}} \quad (1)$$

When the detonation product expands to a certain volume, the first two terms on the right side of the JWL equation are negligible, and the behavior of the detonation product is simulated by the ideal gas state equation: $p = \rho(\gamma - 1)e$, $\gamma = \omega + 1$, The parameters of the equation are shown in Table 3.

Tab.3 TNT state equation parameters

A/kPa	B	R1	R2	ω	E0/ $kJ \cdot kg^{-1}$	\bar{V}_0
3.7377×10^8	3.7471×10^6	4.15	0.9	0.35	6×10^7	1.0

(4)Water

There are Polynomial and shock equations in the material library that comes with the AUTODYN software. Since AUTODYN cannot directly set the hydrostatic pressure, the hydrostatic pressure can only be simulated by setting the internal energy of the water. The polynomial state can set the internal energy of the water, so the polynomial equation of state is chosen for calculation:

$$p = \begin{cases} A_1 u + A_2 u^2 + A_3 u^3 + (B_0 + B_1 u) \rho_0 e & (u > 0, \text{Compressed state}) \\ T_1 u + T_2 u + B_0 \rho_0 e & (u < 0, \text{Stretched state}) \end{cases} \quad (2)$$

In the middle, $u = \frac{\rho}{\rho_0} - 1$, The equation of state before the explosion can be simplified to $p = B_0 \rho_0 e$. The remaining parameters are shown in Table 4.

Tab.4 Water state equation parameter

$\rho/kg \cdot m^{-3}$	G/ $m \cdot s^{-2}$	B_0	A_1/kPa	A_2/kPa	A_3/kPa	T_1/kPa	T_2
1000	9.8	0.28	2.2×10^6	9.54×10^6	1.457×10^7	2.2×10^6	0

1.2. Establishment of finite element model

If the complete process of damage of ice materials under the action of explosion

is calculated, the calculation difficulty will be very large, and it is impossible to investigate the damage effect of various explosive loads on ice materials. The whole process of explosion damage is divided into two major stages: shock wave damage stage and bubble damage stage. The coupling model is established for the two stages, and different working conditions are calculated to explore the damage effect and damage mechanism of each stage. The specific working conditions are set as shown in Table 5, where the dimensionless coefficient $\gamma = \frac{\text{The burst distance}}{\text{The maximum bubble radius}}$.

1.2.1. Establishment of shock wave-ice layer coupling model

According to the distribution position of the ice layer in reality, a three-layer distribution of air layer, ice layer and water layer is used to establish a near-field condition underwater explosion coupling model (shown in Figure 1). In this paper, the CEL method is adopted. The overall size of the Euler domain is 4m×4m. The cell grid is center-encrypted, the minimum mesh size is 0.001m, and the number of cell grids is 360000. The infinite watershed is simulated by the non-reflective boundary condition. The water size is 4m×2.4m, the weight of TNT is 0.023kg, and the radius is 0.015m. The burst distance h and its corresponding dimensionless coefficient are shown in Table 5. The air layer has a size of 4m x 1m and is a standard atmospheric pressure. The ice body adopts Lagrange unit with a total size of 2m*1m, the total number of unit grids is 7.2E4. The infinite domain ice layer is simulated by the non-reflective boundary condition. The artificial viscosity coefficient is adjusted to 0.08 and 1.0 respectively.

1.2.2. Bubble-ice layer coupling model establishment

In the study of the damage effect of bubbles on the ice layer, the damage during the shock wave phase is neglected, and only the influence of the bubble on the non-damaged ice layer is studied. The specific numerical simulation process is as follows: On the basis of the shock wave-ice layer coupling model of each working condition, the ice layer is set as a rigid body and the calculation is started, and the shape of the bubble is recorded; when the bubble is about to be destroyed, the rigid body setting of the ice layer is cancelled to calculate The damage process of the ice layer in the bubble stage (shown in Figure 2).

Tab.5 Calculation of coupled model of underwater near-field explosion

Working condition	1	2	3	4	5	6	7	8	9	10	11
The burst distance/m	1.0	0.8	0.66	0.53	0.47	0.4	0.34	0.29	0.23	0.18	0.13
The dimensionless coefficient / γ	2.44	1.91	1.50	1.29	1.15	1.00	0.83	0.71	0.58	0.44	0.33

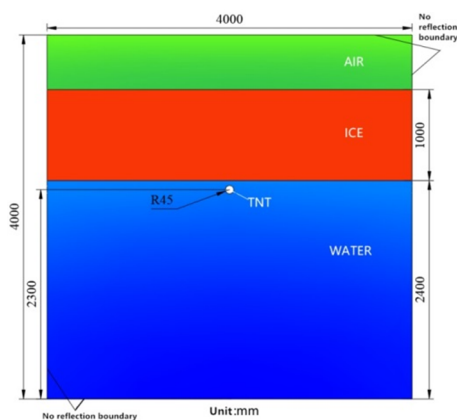


Fig.1 Shock wave -ice coupling model

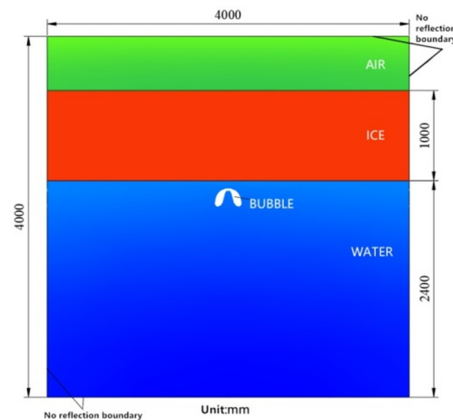


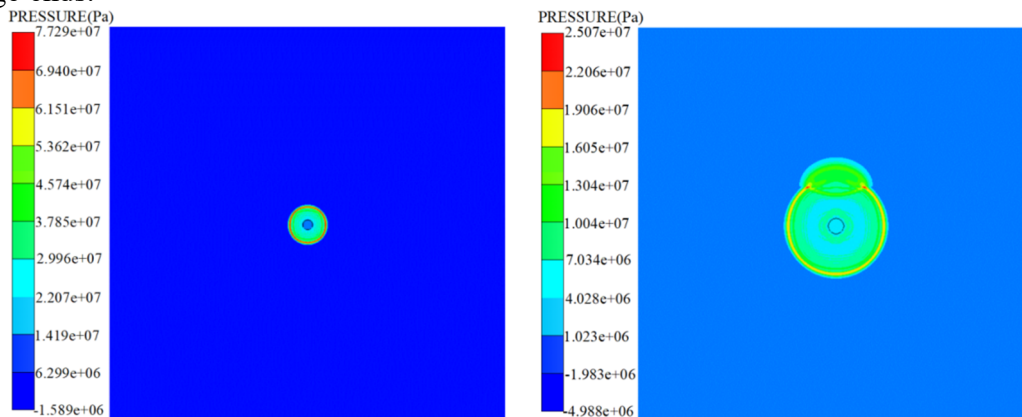
Fig.2 Bubble-ice coupling model

2. Simulation calculation results and analysis

2.1. Ice damage process during shock wave phase

The damage forms of the ice layer in the shock wave stage are mainly divided into two types: the spallation caused by the unloading of stress waves inside the ice layer and the radial cracks formed by the expansion on the layer of cracks.

Numerical simulations and experiments can observe the phenomenon of spallation caused by stress wave unloading and the expansion of radial cracks. Due to the limitations of observation methods, only layer-by-layer thickening can be observed by numerical simulation. The numerical simulation results of working condition 9 (burst distance is 0.23m) are displayed. Taking the TNT explosion time as the initial timing point, Fig. 3-a shows the initial process of shock wave propagation. When $t=0.2$ ms, the detonation shock wave is incident on the ice layer. Under near-field conditions, the stress wave formed by the shock wave entering the ice layer is still spherical (Fig. 3-b, Fig. 3-c, the left is the stress contour map, and the right is the ice damage map, below The illustrations are for this setting). Since the ice material can withstand large compressive stress, the ice layer is not damaged at this time (as shown in Fig. 3-c); when $t=0.5$ ms, the stress wave is reflected on the backburst surface to form a stress wave. In the unloading zone, the tensile stress is greater than the tensile stress limit of the ice material, and the damage begins to occur from the back layer of the ice layer. The main form is spallation and a conical distribution. The spacing of the lobes gradually increases (Fig. 3-d); when $t=1.4$ ms, the stress wave unloading area at the back blast surface expands and expands with the action of stress waves and detonation products over time. The location of the damaged area of the explosion surface is also gradually expanding. At the same time, the stress wave unloading zone also appears in the middle of the ice layer. It can be seen from Equations 11 and 12 that the distribution distance of the stress wave unloading interval at this time has a larger spacing than the backburst surface, and the thickness of the formed cracked piece increases. (Fig.3-e). The multiple spallations of the back-explosion surface continue to expand under the action of stress, gradually forming a cone-shaped damage zone, and the radial crack and the circumferential crack zone begin to expand on the crack that has already appeared (shown in Fig.3-f); when $t=4$ ms, the detonation shock wave has decayed to a lower level, and the oscillation of the internal stress wave on the two free surfaces becomes the main cause of damage. The oscillation of the stress wave causes the stress wave unloading zone to extend to the explosion surface, and the impact surface begins to appear in the same tensile damage zone as the backburst surface damage, but the damage scale is smaller than the backburst surface crack size and the crack thickness is Increase (shown in Fig.3-g). Then the cone-shaped damage area at the top of the ice layer no longer develops, and the damage effect of the shock wave on the ice layer is very limited. It can be concluded that the damage of the ice layer at the shock wave stage ends.



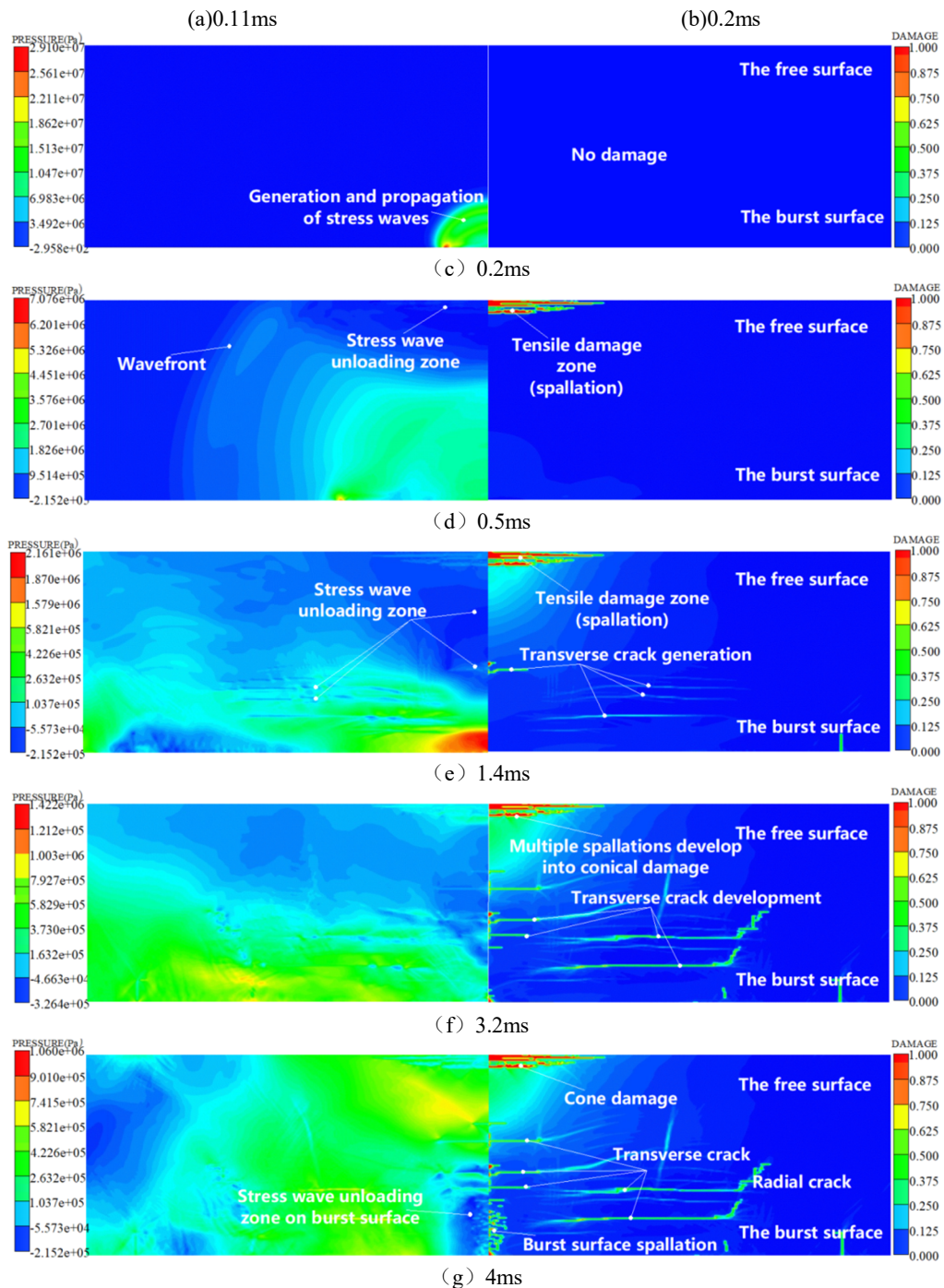


Fig. 3 Stress contour and damage process of ice in shock wave stage

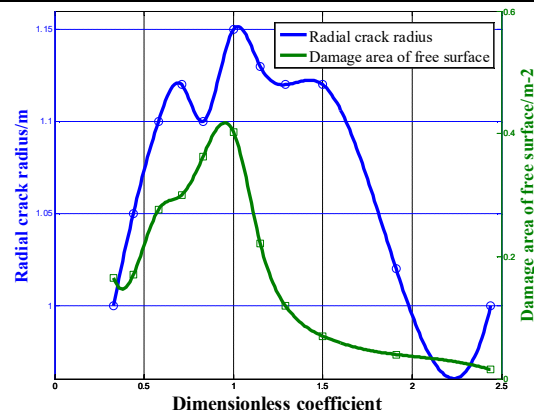
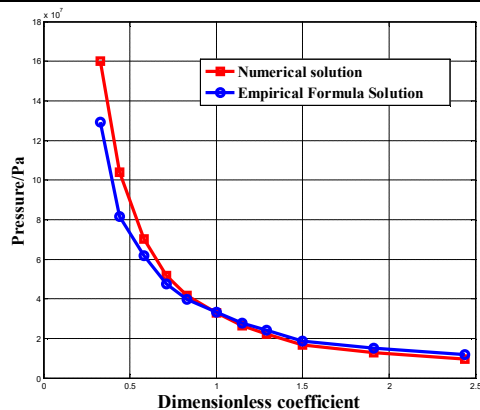
The damage form and development of the other working conditions are similar to those of the working conditions, but the damage range shows a certain regularity with the change of dimensionless coefficient. The damage quantity $D > 0.4$ is defined as effective damage. The damage situation under each working condition is counted as shown in Table 6. Fig. 4-a is a comparison between numerical results and empirical formulas of peak shock waves at different working conditions 0.01M away from the ice blasting surface. It can be seen from the figure that the numerical results are slightly larger than those of empirical formulas when the dimensionless coefficients are small, which is due to the failure of empirical formulas to consider the effect of explosive products; when the dimensionless coefficients are large, the numerical results are slightly smaller than those of empirical formulas, which is due to the larger detonation distance at this time. There is a certain attenuation phenomenon in the numerical results.

Except for extreme conditions, the peak error of shock wave in other conditions is less than 15%, which meets the requirements of Engineering application. Fig. 4-b to Fig. 4-c show the change of the area of conical damage zone, the radius of transverse crack and the area of the damage zone on the blasting face under different dimensionless coefficients. It can be seen that the main damage mode of ice material in shock wave stage is the conical damage of back blasting surface, while the damage degree of transverse crack and frontal blasting surface is lower than that of conical damage, which is the secondary damage mode of ice material in shock wave stage. The simulation results show that the range of each damage zone is the largest when $\gamma=1.0$, and the damage effect on the ice layer is the best. This is due to the fact that the spherical wave formed by detonation does not expand to a certain range when the dimensionless coefficient is small, and the range of incident ice layer is small, which can not form a larger tensile damage zone in the subsequent propagation process, resulting in a larger damage degree but a more concentrated range; and when the detonation distance is large, the shock wave attenuates strongly in water and causes in the ice layer. The stress value is on the low side and the tensile damage zone is small.

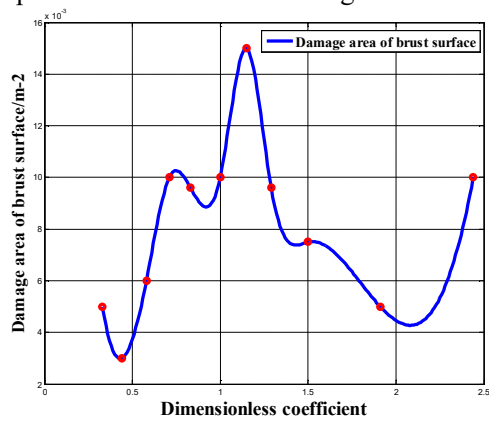
It can be inferred that when the damage area is large, the conical damage area on the back blasting surface will be connected with the damage area on the front blasting surface, resulting in the penetration injury of ice layer in a certain range, which is called "fracture area"; the radial crack and circumferential crack will form a "crack area" with "fracture area" as the center of the circle; and the ice layer outside the "crack area" will be called "crack area" because no damage can be produced." Fig. 4-d is the specific distribution description of each damage area. This is consistent with the damage phenomena of ice under shock wave described in literature^[13].

Tab.6 Ice damage in various conditions during the shock wave phase

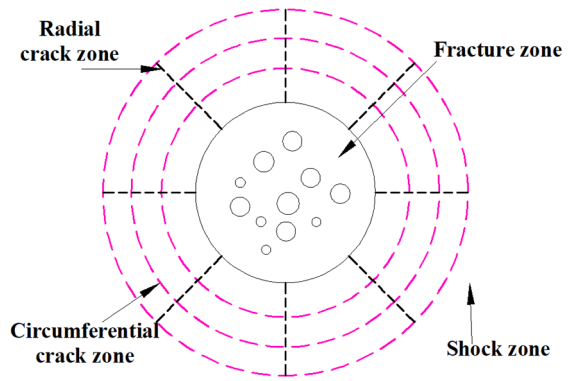
working condition	Burst distance/m	Dimensionless coefficient	Damage area of free surface/m-2	Radial crack radius/m	Damage area of burst surface/m-2	Numerical solution of peak pressure/MPa	Empirical Formula Solution of Peak Pressure/MPa
1	1	2.44	0.015	1.00	0.0100	9.62	11.75
2	0.8	1.91	0.040	1.02	0.0050	12.93	15.12
3	0.66	1.5	0.070	1.12	0.0075	16.69	18.79
4	0.53	1.29	0.120	1.12	0.0096	22.32	24.08
5	0.47	1.15	0.221	1.17	0.0112	26.34	27.58
6	0.4	1	0.403	1.15	0.0100	33.03	33.09
7	0.34	0.83	0.363	1.13	0.0096	41.65	39.76
8	0.29	0.71	0.300	1.12	0.0100	51.75	47.59
9	0.23	0.58	0.276	1.10	0.0060	70.13	61.84
10	0.18	0.44	0.170	1.05	0.0030	100.37	81.58
11	0.13	0.33	0.150	1.00	0.0010	160.14	129.3



(a) Calculation results of shock wave pressure peaks under different working conditions



(b) Calculation results of cone damage area and spallation radius under different working conditions



(c) Calculation results of cone damage area and spallation radius under different working conditions

(d) Destruction of ice layer under shock wave

Fig.4 Statistical calculation of shock wave phase

2.2. Ice damage process during bubble phase

In the bubble damage stage, although the damage range under different working conditions is different, the damage process is the same as the form, and the numerical simulation results of working condition 9 (burst distance is 0.23m) are displayed. Fig. 5-a is a pressure field diagram of the water body when the bubble is broken. At this time, $t=0.1\text{ms}$, it can be observed that the shock wave is generated due to bubble bursting; Fig. 5-b is the pressure field diagram of the shock wave incident on the ice wave at $t=0.115\text{ms}$. At this time, the range of stress waves in the ice layer is small, so the damage of the ice layer is not recorded. When $t=0.116\text{ms}$ (Fig. 5-c), the stress wave range inside the ice layer expands, and the stress wave has a certain degree of dissipation inside the ice layer, and the peak value decreases. It can be observed that there is slight damage to the surface of the ice layer at this time, but the range is small, and the individual unit reaches the compression failure strength, which should be ignored; when $t=2.316\text{ms}$ (Fig. 5-d), the stress wave unloading can be observed. The back layer of the ice layer appeared in the area, and tensile damage began to appear in the stress wave unloading area. The damage form was layer crack, and the thickness of the layer cracks increased and decreased due to the exponential decay of the stress wave. The damage mode is consistent with the damage mode of the back-explosion surface in the shock wave damage stage; when $t=3.000\text{ms}$ (Fig. 5-e), the area of the stress wave unloading area increases continuously, but the tensile stress peak decreases, under the action of stress. The crack that has been generated continues to develop, and a spallation occurs at a portion of the middle portion of the ice layer. At this time, due to the impact of the jet on the ice layer, the compressive stress value of the explosion surface is greatly increased. Under the action of the high pressure stress, some ice layers impacted by the jet on the surface of the ice layer begin to compress and fail, forming crushing damage and overall performance. Similar to penetration. When $t=4.000\text{ms}$ (Fig. 5-f), the peak value of compressive stress generated by the jet impacting the ice layer drops below the compressive failure stress value of the ice material. At this time, the crushing failure zone of the explosion surface has developed to a certain scale. And stop development, the spar cracks that have been generated continue to develop, and on the basis of this, radial cracks are developed. Then the cone damage at the top of the ice layer no longer develops, and the damage of air bubbles to the ice layer is very limited.

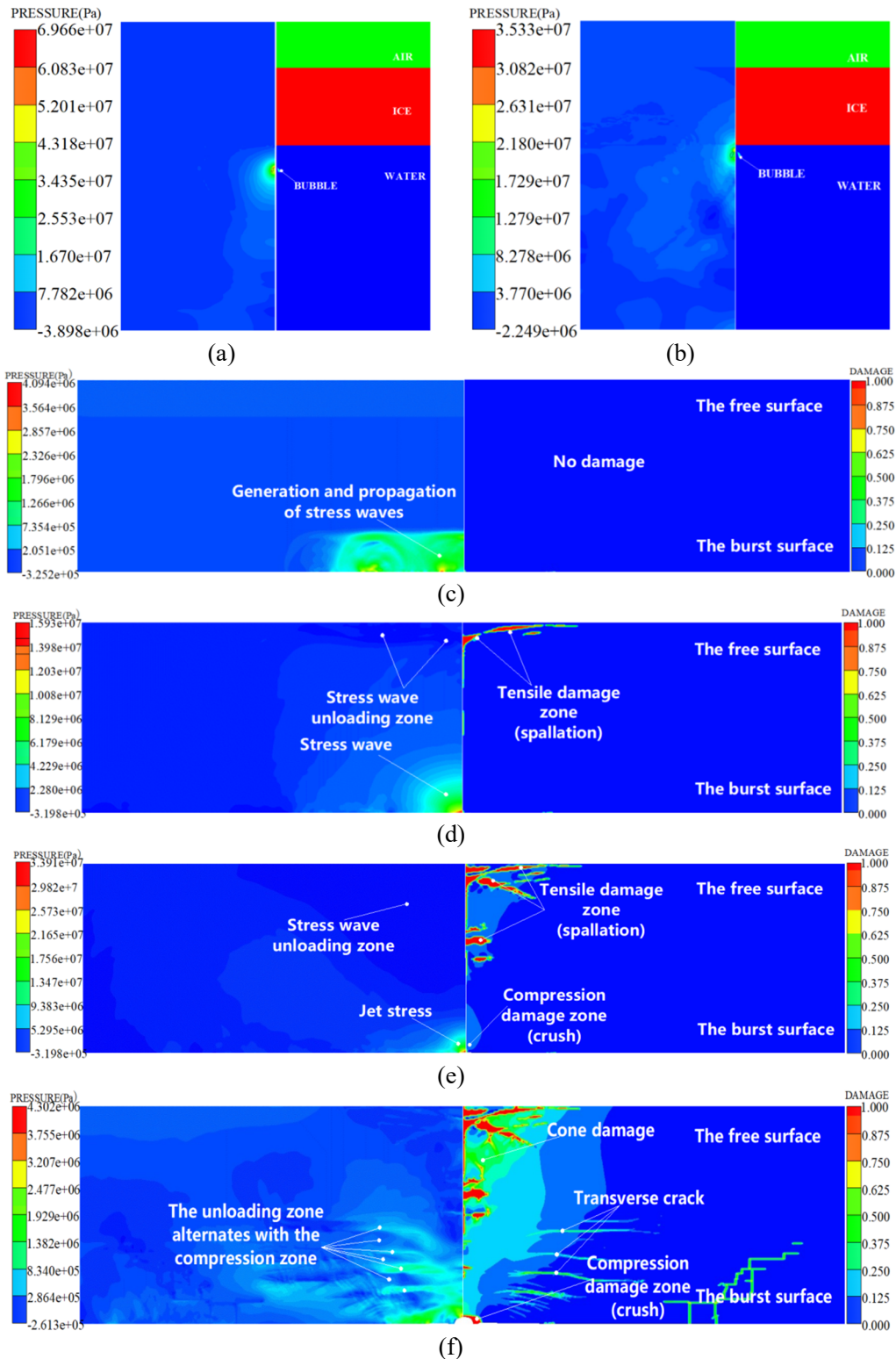


Fig.5 The stress contour and the ice damage process in the ice bubble stage

During the damage process of the ice material in the bubble stage, it is still roughly divided into two parts: the back explosion surface damage and the explosion surface damage. The damage of the back explosion surface is mainly caused by the impact of the bursting of the bubble and the impact of the jet on the ice layer. As the bubble bursts, a shock wave and a jet are formed and impact the ice layer, causing stress waves in the ice layer. The damage process is similar to the damage effect of the shock wave stage, that is, the stress is unloaded at the back explosion surface to cause tensile

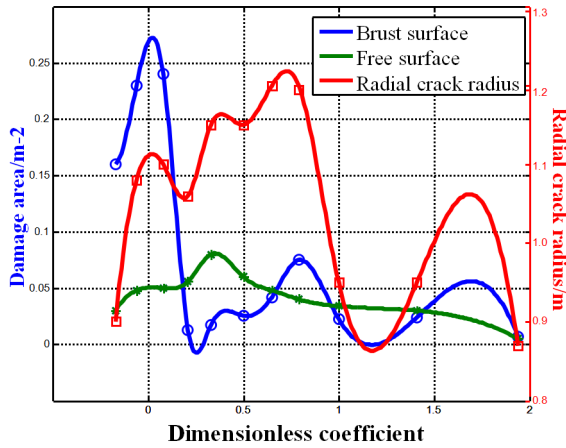
failure and form spallation and radial cracks. However, due to the difference in peak size, incident ice layer range and attenuation form between the bubble burst shock wave and the detonation shock wave, the distribution of the backburst surface crack caused by the two is slightly different, but the whole still maintains the back explosion. Surface cracking - development into a cone-shaped damage - the damage process that occurs and develops by radial cracks.

The damage process of the explosion surface can be roughly divided into two categories: the first type is a shock wave formed in the bursting of the bubble, and a tensile stress zone is formed locally on the impact surface. When the dynamic tensile failure criterion of the ice layer is exceeded, the tensile failure occurs. Causes damage to the ice. The type of loss and the damage process are similar to the impact surface damage in the shock wave phase, and will not be described here. The second type is that under the condition of small dimensionless coefficient, the shock wave formed by bubble burst exceeds the compressive failure strength of the local ice layer on the burst surface and directly causes crushing damage, or the impulse generated when the jet impacts the ice layer is large enough. This causes damage similar to penetration. The specific reason is that, under the condition that the dimensionless coefficient is small, the bubble rupture is larger and the dimensionless coefficient is more severe, the jet is more concentrated, and the number of small bubbles formed after the bubble is broken is reduced. The energy inside the bubble is converted into the internal energy of the shock wave and the jet. The bubble bursting shock wave intensity and the jet impulse are higher, and when the ice layer is impacted, the compressive failure strength of the ice layer can be directly reached and crushed. And when the dimensionless coefficient is small, the damage form is the main form of the bubble damage stage^[10].

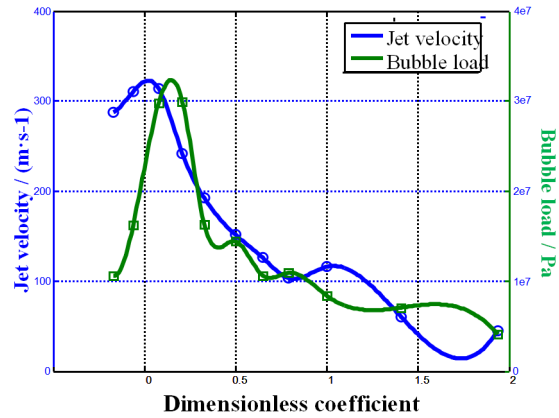
In the remaining conditions, the damage form and development are similar to the working conditions, but the damage range shows a certain regularity with the change of the dimensionless coefficient. The damage with $D > 0.4$ or more is defined as effective damage, and the statistics are under various conditions. The damage is shown in Table 7. Fig. 6-a and Fig. 6-b show the changes in the extent of each damage zone, jet velocity and bubble load under various operating conditions. When the $\gamma = 0.58$ is near, the jet velocity is the largest (about 300m/s), and the damage area corresponding to the explosion surface is also the largest. It can be observed that when the γ is greater than 0.83, the change in the area of the impact surface is small, and when it is less than 0.83, there is a jump increase. This is because the jet velocity is greater than about 200 m/s, and the jet impulse is large. The pressure generated by the impact ice layer will directly exceed the compressive failure strength of the ice material, and the jet has a significant penetration effect on the ice layer; the backburst surface damage area The maximum appears in the vicinity of $\gamma = 0.83$ (condition 7), which is not the attachment of $\gamma = 0.58$ (case 9) with the largest bubble load. This reason is consistent with the cause of the damage of the back-explosion surface in the shock wave stage, and will not be described here. The bubble load and jet do not appear in the condition with the smallest dimensionless coefficient. This is because the dimensionless coefficient is particularly small, the bubble is affected by the ice layer, the jet generation time is short, and the bubble can transform the internal energy of the shock wave and the jet. insufficient. As the dimensionless coefficient increases, the jet generation time is prolonged and each energy conversion is sufficient. When the dimensionless coefficient is further increased, the ice layer is less attractive to the bubble, and the bubble will form a jet after multiple pulsations. The bubble can be consumed in multiple pulsations, and the attenuation effect of the shock wave and the jet propagating in the water is obvious

Tab.7 Ice damage in various working conditions in the bubble stage

working condition	Burst distance/m	Dimensionless coefficient	Damage area of free surface/m-2	Radial crack radius/m	Damage area of burst surface/m-2	Jet velocity / (m·s-1)	Bubble load / Pa
1	1.00	2.44	0.005	0.87	0.0070	45.27	4.07E+06
2	0.80	1.91	0.030	0.95	0.0240	60.53	7.03E+06
3	0.66	1.50	0.034	0.95	0.0225	115.77	8.37E+06
4	0.53	1.29	0.040	1.20	0.0750	103.02	1.09E+07
5	0.47	1.15	0.048	1.20	0.0420	125.78	1.06E+07
6	0.40	1.00	0.060	1.15	0.0255	151.32	1.44E+07
7	0.34	0.83	0.080	1.15	0.0170	192.20	1.63E+07
8	0.29	0.71	0.056	1.06	0.0130	241.55	2.99E+07
9	0.23	0.58	0.050	1.10	0.2400	314.02	2.98E+07
10	0.18	0.44	0.048	1.08	0.2300	310.52	1.62E+07
11	0.13	0.33	0.030	0.90	0.1600	287.62	1.06E+07



(a) Calculation results of each damage area under different working conditions



(b) Calculation results of each damage area under different working conditions

Fig.6 Statistical calculation of Bubble phase

3. Conclusions

1) Underwater explosion The damage process of the ice layer during the whole detonation process is mainly divided into two categories: the shock wave damage stage caused by detonation and the bubble damage stage; the damage mechanism is classified, and the whole detonation process is on the ice layer. Damage can be divided into tensile failure caused by stress wave unloading and crushing failure due to excessive shock wave values.

2) In the shock wave damage stage, the damage of the ice layer is mainly caused by the tensile failure caused by the stress wave unloading of the back explosion surface, and further develops on the basis of the existing damage under the action of the stress wave, forming a cone damage zone and Radial cracks. In addition, the tensile failure of the explosion surface caused by the stress wave oscillation is also one of the damages in the shock wave stage, but the damage degree is lower than that of the back surface damage; in the bubble damage stage, the shock wave generated by the bubble breaking is similar to the explosion shock wave. The form of damage is similar; the jet impacts the ice layer and causes similar penetration damage on the surface of the ice.

3) By comparing the results of the two-stage numerical simulation, it can be seen that the shock wave phase has a large load intensity, the stress wave unloading effect is

more obvious, and the damage range is larger. Therefore, the shock wave phase is the main stage of ice damage caused by underwater explosion. The damage form focuses on the tensile damage of the backburst surface, which is the main damage form of the ice near-field explosion. The bubble stage is the secondary stage of ice damage. The damage form focuses on the penetration damage of the explosion surface, which is the secondary damage form of the underwater near-field explosion to the ice layer.

REFERENCES

1. Xia Changfu. "Research and practice of underwater artificial blasting ice technology", blasting(2014)
2. Shen Wu, Lin Shu. "Strain rate sensitivity of uniaxial compression in eastern Bohai for one year", Journal of Dalian University of Technology(1984)
3. Tong Zheng. "Blasting and explosion technology", Chinese People's Public Security University press(2002)
4. Yan Shichun, Tong Zheng, Wang Hu He, Wang Ping. "Experimental study and numerical simulation of ice body standard blasting crater", engineering blasting(2011)
5. Yin Hui Tang, Yang Xuehai, Jiang Miao, Jin Ji Liang. "Experimental study on blasting ice breaking in extended ice pack under water ice", engineering blasting(2010)
6. Qu Yandong, Liu Wanli, Zhai Cheng, Li Ning. "Numerical analysis of the propagation law of shock wave in underwater explosion explosion breaking", blasting(2017)
7. Wang Huhe, Tong Zheng, Xing Yongming, Li Jinfu. "Mechanism and numerical simulation of explosive crack propagation in infinite ice medium", experimental mechanics(2009)
8. Zhang Zhong, Liang, Liang Qian, Wang Shuli. "Numerical analysis of ice breaking mechanism under underwater blasting", blasting(2015)
9. Philipp A, Lauterborn W. "Cavitation erosion by single laser-produced bubbles", Journal of Fluid Mechanics(1998)
10. Chahine G L, Kapahi A, Choi J K, et al. "Modeling of surface cleaning by cavitation bubble dynamics and collapse", Ultrasonics Sonochemistry(2015)
11. Chao-Tsung H, Jayaprakash A, Kapahi A, et al. "Modelling of material pitting from cavitation bubble collapse", Journal of Fluid Mechanics(2014)
12. Graaf K L D, Brandner P A, Penesis I. "The pressure field generated by a seismic airgun", Experimental Thermal & Fluid Science(2014)
13. Wang Ying, Xiao Wei, Yao Xiongliang, Qin Yezhi. "The characteristics of ice fracture and its influencing factors under the impact of underwater explosion shock wave". Explosion and impact(2018)
14. Cui P, Zhang A M, Wang S, et al. "Ice breaking by a collapsing bubble", Journal of Fluid Mechanics(2018)
15. Cui X, Yao X, Chen Y. "A Lab-Scale Experiment Approach to the Measurement of Wall Pressure from Near-Field under Water Explosions by a Hopkinson Bar"(2018)
16. Chen Y, Yao X, Cui X. A Numerical and Experimental Study of Wall Pressure Caused by an Underwater Explosion Bubble[J]. 2018.
17. Liu, L. T., X. L. Yao, A. M. Zhang, B. S. Sun, Research on the estimate formulas for underwater explosion bubble jet parameters[J]. Ocean Engineering, 2018. 164: p. 563-576.